

# RESISTIVE-WALL INSTABILITY IN THE DAMPING RINGS OF THE ILC\*

L. Wang<sup>#</sup>, K.L.F. Bane, T. Raubenheimer and M. Ross, SLAC, Menlo Park, CA, USA

## Abstract

In the damping rings of the International Linear Collider (ILC), the resistive-wall instability is one of the dominant transverse instabilities. This instability directly influences the choice of material and aperture of the vacuum pipe, and the parameters of the transverse feedback system. This paper investigates the resistive-wall instabilities in an ILC damping ring under various conditions of beam pipe material, aperture, and fill pattern.

## INTRODUCTION

The baseline design of the ILC Damping Rings consists of one 6km ring for the electron beam and two 6km rings for the positron. The alternative is a 17km ring to accommodate as many bunches as possible and to allow long gaps for ion clearing (in the electron-damping ring). This paper estimates the resistive-wall instability of the baseline, 6km ring.

Table 1 shows the key parameters of one 6km damping ring. Its betatron functions are shown in Figure 1. There are 8 wiggler sections, 10 ARC sections and 2 long straight sections. The vacuum chamber in the wiggler section has a small vertical aperture (16mm in the optimized design). As a result, the resistive wall impedance of the vacuum chamber can become significant. Besides aluminium, stainless steel also is an option for the material of the vacuum chamber (due to its lower outgassing rate). A third option for the chamber material, copper-coated stainless steel, is also considered, in order to reduce both the resistive wall impedance and the outgassing rate. There are various bunch fill patterns in the damping ring, which depend on the timing system and the RF system. In this paper, a numerical program is used to simulate the resistive-wall instability in the 6km ring with various options of fill pattern, aperture, and material of the vacuum pipe.

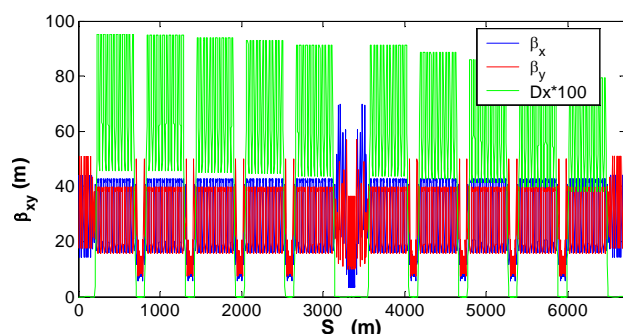


Figure 1 Betatron function of the 6km damping ring.

\*Work performed under the auspices of the U.S. Department of Energy under contract DE-AC02-76SF00515

<sup>#</sup> electronic address: wanglf@slac.stanford.edu

Table 1 The main parameters of a 6km ring

Description	Value
Beam energy	5.0 GeV
Circumference	6695 km
Harmonic number	14516
RF frequency	650 MHz
Tunes	52.28/47.40
Momentum compaction	$0.40 \times 10^{-3}$
Number of bunches	2767~5782
Bunch intensity	$0.97 \sim 2.02 \times 10^{10}$
Emittance at injection	$5.0 \times 10^{-10}$ m
Average betatron function	22.5m

## RESISTIVE WALL IMPEDANCE

### Pure aluminium or stainless steel chamber

The resistive-wall instability depends on the aperture and material of the vacuum of chamber. The standard transverse impedance of a thick wall of length  $L$  is give by [1]

$$Z_{\perp}(\omega) = (1 - i \operatorname{sgn}(\omega)) \frac{L Z_0}{2\pi b^3} \sqrt{\frac{2c}{Z_0 \sigma}} \frac{1}{\sqrt{|\omega|}} \quad (1)$$

Here  $Z_0$  is the impedance of free space,  $b$  the radius of the beam pipe,  $\sigma$  the conductivity of the pipe material and  $c$  the speed of light. A round chamber is assumed in this paper. A more realistic mode about shape of chamber will be studied in the future. The wake function corresponding to (1) is

$$W_{\perp}(s) = \frac{cL}{\pi b^3} \sqrt{\frac{Z_0}{\pi \sigma}} \frac{1}{\sqrt{s}} \quad (s > 0) \quad (2)$$

Aluminium is a preferred option with a large conductivity of  $3.773 \times 10^7 \Omega^{-1} \text{m}^{-1}$ . Stainless steel has a lower conductivity of  $1.37 \times 10^6 \Omega^{-1} \text{m}^{-1}$ . The impedance of the Aluminium chamber is a factor of 5.25 small than that of stainless steel one. However, stainless steel has a lower outgassing rate.

### Copper-coated stainless steel chamber

For a two-layer beam pipe, when the frequency is low enough so that the thickness of the high-conductivity layer is smaller than its skin depth, the impedance is modified by a multiplicative factor. The long-range resistive wall impedance of a stainless steel chamber coated with copper is given by [2, 3]

$$Z_{\perp}(\omega) = \xi(\omega) (1 - i \operatorname{sgn}(\omega)) \frac{L Z_0}{2\pi b^3} \sqrt{\frac{2c}{Z_0 \sigma_1}} \frac{1}{\sqrt{|\omega|}}, \quad (3)$$

$\sigma_1$  is the conductivity of copper ( $5.977 \times 10^7 \Omega^{-1} \text{m}^{-1}$ );  $\xi$  is a correction factor that takes into account the effect of the stainless steel

$$\xi(\omega) = \frac{1 + \sqrt{\sigma_2 / \sigma_1} Z_1(\omega) Z_2(\omega)}{Z_1(\omega) + \sqrt{\sigma_2 / \sigma_1} Z_2(\omega)} \quad (4)$$

with  $\sigma_2$  is the conductivity of stainless steel;  $Z_1$  and  $Z_2$  are given by

$$Z_k(\omega) = \frac{1 - \exp[-2(1-i)t_k / \delta_k(\omega)]}{1 + \exp[-2(1-i)t_k / \delta_k(\omega)]}, \quad (5)$$

with  $t_k$  the thickness of the  $k$ th layer and  $k=1, 2$  for the copper and stainless steel layers, respectively. For high frequencies with  $t_k > \delta_k$ , the factor  $\xi$  is 1 ( $\delta$  is the skin depth),

$$\delta(\omega) = \sqrt{2} / \sqrt{\mu_0 \sigma |\omega|} \quad (6)$$

The lowest frequency of interest for the resistive-wall instability is  $q$  times the revolution frequency  $\omega_0 = 0.28135$  MHz. Here  $q$  is the fractional part of the betatron tune, which is 0.28 and 0.4 in the horizontal and vertical directions. The skin depth at this low frequency is 0.58 and 0.48 mm. A thickness of 0.1mm copper is assumed, which corresponds to a shielding frequency (where  $t=\delta$ ) of  $\omega/2\pi = 0.45$  MHz. Above 0.45 MHz, the impedance is basically determined by the copper layer, while below it, the impedance is influenced by the stainless steel as shown in Figure 2.

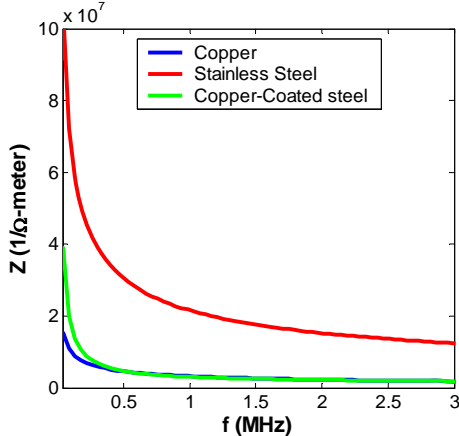


Figure 2 Real part of impedance for stainless steel, copper and copper-coated stainless steel.

## PHYSICAL MODEL

Program SCBI (Simulation of Coupled Bunch Instabilities) is a three-dimensional program for tracking particles through a storage ring with various impedances (wake fields). The distribution of impedances, such as RF cavities along the ring, can be modelled according to a realistic design. At each element (impedance source), the bunch receives a kick from the wake field generated by previous bunches. In this study, the effective resistive wall impedance along the ring is calculated and then located at one position in order to speed up the calculation.

The resistive wall instability is not sensitive to the beam fill pattern in our case. Two fill patterns are considered in this study. One fill pattern has a smaller number of bunches, 2767, but a higher single bunch

population  $N = 2.02 \times 10^{10}$ . The whole beam consists of 61 trains of 23 bunches and 62 trains of 22 bunches. The bunch spacing is 4 RF buckets and the train gap is 28 RF buckets. Another fill pattern we consider here has 5782 bunches with  $N = 0.97 \times 10^{10}$ . There are 118 trains with 49 bunches per train. The bunch spacing is 2 RF buckets and the train gap is 25 RF buckets.

The resistive wall instability is very sensitive to the vacuum chamber aperture (see Eq. 1). The aperture also affects the acceptance, cost, electron cloud effect, vacuum and BPM performance. Three proposed options for the beam pipe aperture are shown in Table 2.

Table 2 Options of the pipe aperture  $b$  (mm)

	Option I 44/16/100	Option II 50/32/100	Option III 50/46/100
ARC	44	50	50
Wiggler	16	32	46
Straight	100	100	100

## RESULTS

Table 3 shows the growth time under various conditions.

### Beam fill pattern effect

The gap between bunch trains is 38 ns and 43 ns for the 2767 and 5782 bunches fill patterns, respectively. The two fill patterns have the same total beam current. Because the resistive-wall wake field decays slowly as  $1/\sqrt{s}$ , it provides coupling over many turns. As a result, the instability is similar for different beam fill patterns.

### Vacuum chamber aperture effect

The resistive wall impedance is inversely proportional to the cube of the aperture. There is a small aperture 16mm in the wiggler section of Option I. The impedance of the wiggler section dominates in this case. The difference in the instability growth time between Option II and III is smaller. Option I with a stainless steel chamber has the shortest growth time 8 turns. All other options have growth times longer than 20 turns.

### Vacuum pipe material effect

With an aluminium beam pipe, a small pipe aperture (Option I) can be chosen. However, aluminium has large secondary electron yield (SEY) and the electron cloud density usually is higher with a smaller pipe aperture. If stainless steel is the choice, the aperture of the beam chamber would better be Option II. A 0.1mm copper-layer on stainless steel can suppress the resistive-wall instability by a factor of 4.0. Figure 3 shows the growth of the bunch oscillation amplitude for the case of stainless steel and copper-coated stainless steel vacuum pipes. If copper-coated stainless steel is used, the growth time will be longer than 35 turns even with the smallest wiggler aperture (Option I). Copper-coated stainless steel combines many advantages such as reducing outgassing, the impedance, SEY, cost, etc.

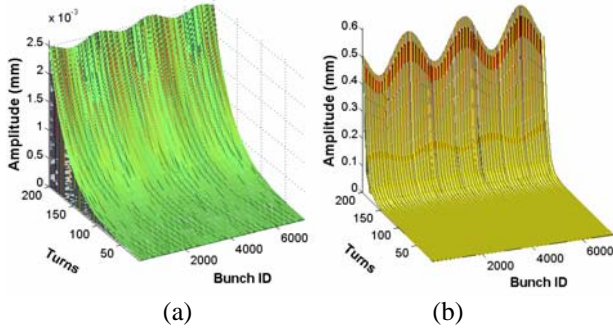


Figure 3 Growth of bunch oscillation amplitude with copper-coated stainless steel (a) and stainless steel (b) vacuum pipes. Aperture pattern is Option I and the number of bunches is 5782.

### Fractional part of the betatron tune

The effective transverse impedance is sensitive to the fraction part of the betatron tune  $q$ . Figure 4 shows the growth in beam amplitude with different  $q$ . With integer and half integer  $q$ , the amplitude grows linearly, instead of exponentially, with time. The growth time decreases from 41 to 36 turns when  $q$  changes from 0.1 to 0.4.

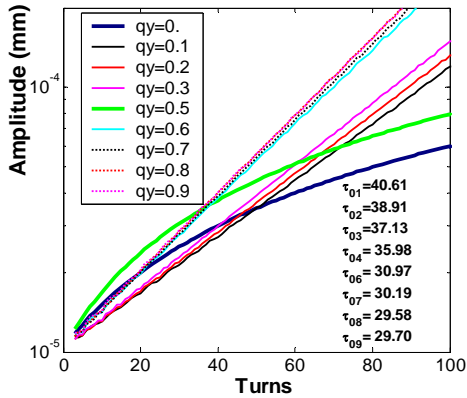


Figure 4: Amplitude growth for different of fractional betatron tune. Copper-coated stainless steel, 2676 bunches, aperture option I.

### Bunch-by-bunch feedback system

Bunch-by-bunch feedback will be applied to suppress the resistive-wall instability. The required feedback bandwidth is 320 MHz (1.0/bunch spacing) with a damping time 0.4~0.8ms, which is close to the feedback damping time of 0.5 ms in the B-factories. Figure 5 shows the feedback effects upon the unstable modes in the case of a copper-coated chamber with aperture Option I. The feedback is turned on at the 100<sup>th</sup> turn. The resistive-wall instability growth time is 0.8ms. A feedback gain of 0.67ms can suppress the instability.

The feedback kicker voltage is maximum at beam injection time where the beam has a large oscillation. Assuming a betatron function at the feedback kicker  $\beta=22.59\text{m}$ , damping time of 0.4 ms and a requirement of one sigma offset at injection, this implies a voltages of 2 kV.

In the electron ring, the fast ion instability has a similar growth time or even faster. To handle the two instabilities together, the required feedback damping time will be around 0.2 ms.

Table 3 Growth time in turns

Material	No. bunches	Option I	Option II	Option III
Stainless Steel	5782	8.73	20.82	22.95
Stainless Steel	2767	8.67	20.70	22.78
Aluminium	5782	45.81	109.26	120.44
Aluminium	2767	45.50	108.6	119
Copper-Coated S.S.	5782	36.26		
Copper-Coated S.S.	2767	35.98		

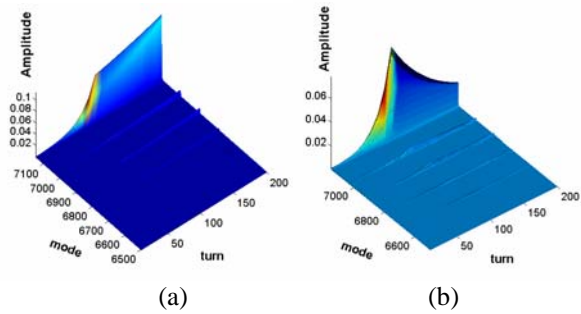


Figure 5 Instability Modes with feedback gain 40turns/0.89ms (a) and 30turns/0.67ms (b). The feedback was turned on at the 100<sup>th</sup> turn. Copper-coated stainless steel with aperture Option I.

## SUMMARY

The resistive-wall instability in the ILC damping ring has been studied for different parameters. As expected, the instability is not sensitive to the beam fill-pattern. The resistive-wall instability due to the wiggler section is dominant when its aperture is small. The feedback system requires a growth time longer than 20 turns (0.45ms), therefore, a larger pipe aperture (Option II) should be considered when pure stainless steel is used. The growth time for aluminium is longer than 45 turns even with small aperture in the wiggler section. However, aluminium has a larger outgassing rate and SEY. Copper-coated stainless steel has all advantages: a longer growth time (>35turns/0.78ms), a lower outgassing rate and SEY.

## ACKNOWLEDGEMENT

The authors gratefully thank Prof. Alex Chao for introducing the impedance model of coated-layers and Dr. S. Heifets for useful discussion.

## REFERENCES

- [1] A. Chao, Physics of Collective Beam Instabilities in High Energy Accelerators.
- [2] J.D. Jackson, SSC Central Design Group Internal Report No. SSC-N-110 (1986)
- [3] E.D. Courant and M. Month, Brookhaven National Laboratory Report No. BNL-50875 (1978)